Arabian Journal of Chemistry (2010) **3**, 121–126

King Saud University

Arabian Journal of Chemistry

www.ksu.edu.sa
www.sciencedirect.com

ORIGINAL ARTICLE

The pristine and carbon, silicon or germanium-substituted (10, 0) BN nanotube: A computational DFT study of NMR parameters

Temer S. Ahmadi [a], **Ahmad Seif** [b,*], **Goodarz M. Rozbahani** [b]

[a] *Department of Chemistry, Villanova University, Villanova, PA, USA*
[b] *Nanoscience Computation Lab, Islamic Azad University, Boroujerd Branch, Boroujerd, Iran*

Received 16 November 2009; accepted 1 January 2010
Available online 10 February 2010

KEYWORDS

Boron-nitride nanotube;
Carbon, silicon and germanium-doped;
Density functional theory;
Nuclear magnetic resonance

Abstract The geometrical structure and nuclear magnetic resonance (NMR) parameters of the pristine as well as carbon, silicon and germanium-doped (10, 0) boron-nitride (BN) nanotubes have been studied using a DFT-B3LYP method for the first time. When either a Ge, C or Si atom is substituted for a single B or N in the BN nanotube, the dopant atom extends outward from the surface of the nanotube. Our results show that Ge extends more from the surface than C or Si. It was found that the NMR parameters are significantly changed for those B and N nuclei that bond directly to C, Si or a Ge dopant. The calculations were carried out using the Gaussian 03 software package.

1. Introduction

Since carbon nanotubes (CNTs) were discovered by Iijima (1991), research on the synthesis and properties of carbon and other nanometer-scale tubular structures have proliferated because these materials offer new opportunities in science and engineering. Among all types, group III-nitrides have gained a wide range of attention due to their unique and attractive properties as well as potential applications. Although many group III-nitride nanotubes have been studied theoretically, only some have been observed experimentally; those include single-walled and multi-walled boron-nitride nanotubes (Bengu and Marks, 2001; Chopra et al., 1995; Loiseau et al., 1996; Golberg et al., 1999; Czerw et al., 2003). BN nanotubes (BNNTs) are inert to oxidation and thus making them appropriate for high temperature use – a major advantage over graphite ribbon and carbon nanotubes. Also, boron-nitride nanotubes are semiconductors while carbon nanotubes can be either metallic or semiconductor depending on the diameter and chirality of the latter (Saito et al., 1998; Blase et al., 1994; Xiang et al., 2003; Wu et al., 2005). Because of their attractive physical properties, BNNT and doped-BNNTs have been studied theoretically.

---

* Corresponding author.
E-mail address: Ahmaseif@yahoo.com (A. Seif).

1878-5352 © 2010 King Saud University. All rights reserved. Peer-review under responsibility of King Saud University.
doi:10.1016/j.arabjc.2010.02.008

Production and hosting by Elsevier

Specifically, three groups (Wu et al., 2005; Si and Xue, 2006; Wu and Zhang, 2008) have performed ab initio calculations on carbon-, silicon-, and germanium-substituted BN nanotubes recently. Their results show that C, Si, and Ge replacements can induce spontaneous magnetization with none, some or very extended deformation in the nanotube, respectively – although the outer shell configuration of the three elements are the same.

Nuclear magnetic resonance (NMR) is a theoretically complex yet simple powerful analytical tool (Bovey, 1988). Although NMR probes the nuclei of atoms and not the electrons, the chemical environment of specific nuclei can be deduced from their NMR information. The chemical shielding (CS) tensors, which are experimentally measured as chemical shift by NMR, arise at the electronic sites of magnetic nuclei in order to prevent the nuclei from feeling the full strength of the applied external field. Although experimental studies are essential in obtaining information about local bonding environment and electronic structure, theoretical calculations can complement our understanding of experimental NMR parameters as has been shown previously in the case of carbon nanotubes where NMR parameters have assisted to determine and distinguish structures of nanotubes (Tang et al., 2000; Goze Bac et al., 2001; Zurek et al., 2007; Hayashi et al., 2003). In the case of BN nanotubes, nuclei of ^{15}N and ^{11}B are detected by NMR and hence calculation of the NMR parameters would be useful to fully understand the local environment of atoms within those nanotubes.

In this work, the pristine and C-, Si-, and Ge-substituted (10, 0) BN nanotube have been studied using density functional theory (DFT) in order to evaluate the influence of C, Si and Ge dopants on the chemical shift tensors at the sites of ^{11}B and ^{15}N for the first time. The length and location of substituted atoms in the (10, 0) BN tubes are similar to the systems of previous investigations by others which were performed to study other properties such as geometry and band structure of the above-mentioned models (Wu et al., 2005; Si and Xue, 2006).

2. Models and computational methods

In order to investigate the influence of substituted C, Si and Ge on the chemical shift tensors at the sites of ^{11}B and ^{15}N in the (10, 0) BN nanotubes, calculations were performed based on the density functional theory (DFT) using the Gaussian 03 program (Parr and Yang, 1989; Frisch et al., 2004). We considered seven models of (10, 0) zigzag single-wall BNNTs with a length of 1.0 nm. Model No. 1 (pristine) is a (10, 0) BN nanotube consisting of 40-B and 40-N atoms forming eight layer of atoms along the tube axis (Fig. 1). Models No. 2–7 are a C-, Si-, and Ge-substituted (10, 0) BNNT where dopant atoms replace either the boron or the nitrogen atom in a (10, 0) BN nanotubes, respectively (Figs. 2 and 3). In each of the models considered in this study, both portals were capped by 20 H atoms in order to avoid dangling bonds and minimize the calculation time; other elements such as Li could be used as well but calculation time would increase with such a choice (Xin et al., 2005). The dopant sites in (10, 0) nanotube are labeled as S_B or S_{ON} as shown in Fig. 2.

Initially, structural optimization is completed for the pristine model and the six possible substitution sites of the C, Si and Ge atoms replacing either the B or the N atom in a boron-nitride nanotube. All structures were optimized using the hybrid density functional B3LYP-DFT. Then, natural population analysis (NPA) and the quantum chemical calculations were carried out on the seven geometrically optimized models by the above-mentioned method; 6-31G(d) standard basis sets (Becke, 1993; Zhang et al., 2005) were used to evaluate natural charges and the ^{11}B and ^{15}N NMR parameters.

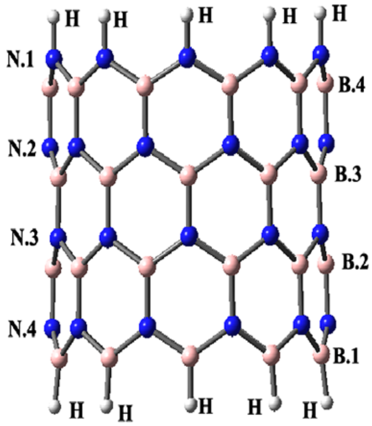

Figure 1 The 2D view of the pristine (10, 0) BN nanotube.

Quantum chemical computations yield the chemical shift (CS) tensors in the principal axes system (PAS) by the order of $\sigma_{11} < \sigma_{22} < \sigma_{33}$. The isotropic chemical shielding (ICS) is determined by $(\sigma_{11} + \sigma_{22} + \sigma_{33})/3$ and the anisotropic chemical shielding (ACS) is calculated using $\sigma_{33} - \sigma_{11} + \sigma_{22}$ (Seif and Boshra, 2009).

3. Results and discussion

The geometrical structure, ICS and ACS parameters of the pristine (10, 0) BN nanotube consisting of 40-B and 40-N atoms as well as mono-substituted (10, 0) BN nanotube were studied; the substitution was made with either a C, Si or a Ge atom at either the boron (S_B) or nitrogen (S_N) site. We found that the local symmetry for all of the samples of the tube breaks up after relaxation, since the C, Si and Ge atoms extend outward from the surface of the normal BN nanotube, forming a tetrahedral structure with the three nearest neighboring atoms. The optimized bond lengths and bond angles for the pristine and C, Si and Ge-doped BNNT are listed in Table 1. The average B–N bond length is 1.47 Å for the pristine form which is in agreement with previous study (Boshra and Seif, 2009). For the S_N substituted form, the bond lengths between C-dopant and three neighboring B atoms (B.23, B.24, and B.34) are 1.54 Å, 1.54 Å and 1.53 Å and for Si- and Ge-dopant with the same neighbors, bond lengths are 1.98 Å, 1.98 Å, 1.96 Å, 2.05 Å, 2.05 Å and 2.02 Å, respectively. The dopant bond with B.23 and B.24 are longer than dopant-B.34 bond because the former bonds include π bonding component. Although the method we used in this work for the optimization of Si- and Ge-doped BNNT is different from that used by others, our values for average bond lengths are roughly the same as references 10 and 11, who found 1.93 Å and 1.97 Å, respectively, for their average dopant-neighboring B-atom bond lengths.

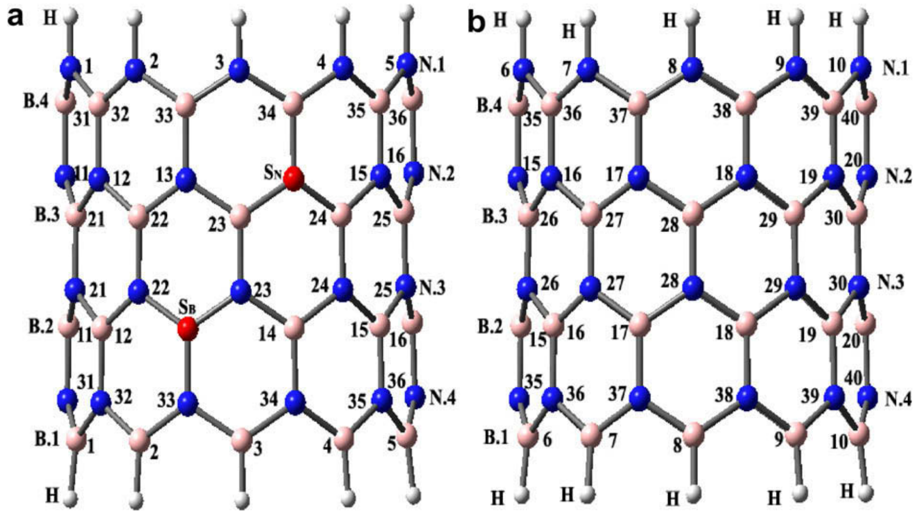

Figure 2 The schematic diagram of boron-nitride nanotube (10, 0), magenta and blue spheres are boron and nitrogen atoms, respectively. Two substitutional sites S_B and S_N (red spheres) for carbon, silicon and germanium atoms. (a) The front side and (b) the back side.

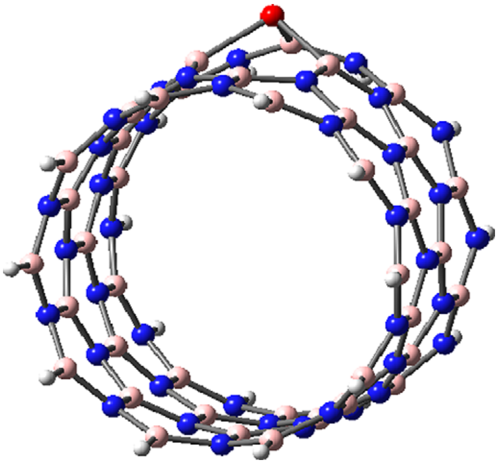

Figure 3 The 3D view of Ge-substituted (S_N) (10, 0) BNNT.

Table 1 Structural parameters of pristine and C, Si and Ge-doped BN nanotubes (10, 0), two substitutional sites S_B and S_N as well as their neighbors are indicated in Fig. 2.

Nuclei	Pristine	S_N[a]
N–B.34	1.47 Å	1.53 Å, [1.96 Å], (2.02 Å)
N–B.23	1.47 Å	1.54 Å, [1.98 Å], (2.05 Å)
N–B.24	1.47 Å	1.54 Å, [1.98 Å], (2.05 Å)
∠B.34NB.24	119.67°	119.50°, [101°], (98.00°)
∠B.34NB.23	119.67°	119.50°, [101°], (98.00°)
∠B.23NB.24	116.90°	115.00°, [94°], (91.00°)
B–N.22	1.47 Å	1.45 Å, [1.77 Å], (1.90 Å)
B–N.23	1.47 Å	1.45 Å, [1.77 Å], (1.90 Å)
B–N.33	1.47 Å	1.42 Å, [1.76 Å], (1.89 Å)
∠N.22BN.23	118.62°	114.37°, [103.43°], (99.00°)
∠N.22BN.33	120.10°	118.00°, [106.37°], (103.00°)
∠N.23BN.33	120.10°	118.00°, [106.37°], (103.00°)

[a] In each row, the first number is for C-doped, the second for Si-doped, and the third for Ge-doped forms of (10, 0) BNNTs.

In the final optimized geometries, bond angles (B.34–S_N–B.24, B.34–S_N–B.23 and B.23–S_N–B.24) decrease slightly in the C-doped model from their original values of 119.67°, 119.67° and 116.90°. This reduction of the bond angles gets persists when Si or Ge is substituted for a nitrogen atom with the latter having the largest decrease in angles – up to 24°. In each of the three substituted systems, B.23–S_N–B.24 bond angles are found to be the smallest of all other bond angles (Table 1). In the case of S_B dopants, the bond lengths between dopants C, Si or Ge and their three adjacent atoms (N.22, N.23 and N.33) are shorter than S_N substituted dopants; these values are also in agreement with the previously reported results (Wu et al., 2005; Si and Xue, 2006). Our results reveal that in the Ge-doped model of BNNT, the Ge–N and Ge–B bond lengths have the largest values and the B–Ge–B and N–Ge–N bond angles have the smallest value in comparison to other doped systems. Table 1 indicates that the order of bond lengths is: Ge–B > Ge–N > Si–B > Si–N > C–N > C–B.

Table 2 shows the evaluated NMR ICS and ACS parameters for ^{15}N and ^{11}B in the pristine model of (10, 0) BNNT. It shows that the 40 B and 40 N atom-nanotube is divided into four layers with equivalent ^{15}N and ^{11}B NMR parameters for each layer which was observed previously as well (Zhang et al., 2005). The ICS values decrease (167, 139, 137 and 104 ppm) going from N.1 to N.4 layers. The ICS values increase (73, 81, 81 and 84 ppm) going from B.1 to B.4 layers. These trends imply that N-mouth has the largest ICS value (highest electronic density) and smallest ACS value while B-mouth has the smallest ICS value (lowest electronic density) and the largest ACS value among all other layers. The NMR parameters of the two portals are totally dissimilar from those of the middle layers of the tube because of the sudden variation of N.1 and B.1 environments due to the presence of hydrogen atoms. Although the choice of basis set used in this work (6-31G(d)) is different from our previous work (6-31G(d, p)) Zhang et al., 2005, the final results are almost the same for both sets used for computation of the NMR parameters. Our results indicate that the calculated NMR parameters are

Table 2 The NMR parameters of the pristine (10, 0) BNNT.

Layers	ICS (ppm)	ACS (ppm)	Layers	ICS (ppm)	ACS (ppm)
N.1	167	74	B.1	73	48
N.2	139	174	B.2	81	34
N.3	137	181	B.3	81	33
N.4	104	230	B.4	84	34

only somewhat sensitive to the choice of basis sets in the density functional theory (Schleyer and Mar, 1996).

First time calculation of the NMR parameters for a C, Si or Ge-doped (10, 0) BNNT with a dopant replacing an N atom (S_N models) or a B atom (S_B models) is shown in Tables 3 and 4. The NMR values for those B atoms (B.23, B.24 and B.34) which are directly connected to a C, Si or a Ge atom in a S_N model show significant changes. The NMR values of those atoms not directly connected to the dopant atom do not undergo any significant changes and their values are the same as those of the pristine model. The ICS values for B.23, B.24 and B.34 in that order are: 75, 75 and 81 ppm (for C-doped); 61, 61 and 68 ppm (for Si-doped); and 60, 60 and 67 ppm (for Ge-doped). The ACS values for the same B nuclei increased with respect to other B nuclei. In other words, those three B atoms have the smallest ICS values in the Ge-doped (10, 0) BNNT when compared with C- and Si-doped models. On the other hand, for those three B atoms which are directly connected to dopant atoms, the ICS values decrease with decreasing bond angles and increasing B–C, B–Si and B–Ge bond lengths. An important point to note is that both B.23 and B.24 nuclei, which are in symmetrical positions, have the same NMR parameters for all of the three models – C, Si or Ge-doped BNNT. Meanwhile, the ICS values of B.34 nuclei are larger than those of B.23 and B.24 nuclei because bond angles between B.23 and B.24 are smallest of all bond angles (Table 1).

The NMR values at the sites of ^{15}N nuclei (N.3, N.4, N.13, N.15, N.23 and N.24) which are directly bonded to B.23, B.24 or B.34 nuclei (C, Si or Ge-bonded) undergo significant changes among the ^{15}N nuclei in comparison with the pristine model. For those ^{15}N nuclei, the ICS values decreased but ACS values increased with respect to the pristine model – changes in the NMR parameters at the site of ^{15}N nuclei due to the presence of lone pair of electrons are more than that at the ^{11}B nuclei. For the S_B model, the NMR parameters (ICS and ACS) for N.22, N.23 and N.33, which are directly bonded to C, Si, or Ge nuclei, demonstrate major changes while other N atoms which are not directly bonded to the dopants undergo smaller changes. It is noted that the changes of the NMR parameters at the sites of ^{15}N nuclei are singularly observed in the front side of nanotube as shown in Fig. 2(a) while those of the back side remained almost unchanged as shown in Fig. 2(b). The ICS and ACS values for N.22, N.23 and N.33 decreased in comparison to the pristine model – in agreement with decreasing bond angles (See Tables 1 and 4).

In the S_B models, changes in the NMR parameters for B atoms located in the front side of the nanotube are minor compared to B atoms of the back side which remained unchanged. In the S_N models, the NMR parameters of both ^{15}N and ^{11}B nuclei in the front side of nanotube are changed. In the S_B models, the NMR parameters changed only at the site of

Table 3 The NMR parameters of C, Si and Ge-substituted (S_N) BNNTs.

Layers	Nuclei	ICS[a] (ppm)	ACS[a] (ppm)	Layers	Nuclei	ICS[a] (ppm)	ACS[a] (ppm)
N.1	1 = 6 = 7 = 8 = 9 = 10	167, [167], (167)	74, [73], (74)	B.1	1 = 2 = 3 = 4 = 5 = 6 = 7 = 8 = 9 = 10	73, [73], (73)	48, [48], (48)
	2 = 5	162, [159], (155)	73, [68], (68)				
	3 = 4	155, [141], (143)	85, [80], (72)				
N.2	11 = 12 = 16 = 17 = 18 = 19 = 20	139, [139], (140)	174, [174], (174)	B.2	11 = 12 = 13 = 15 = 16 = 17 = 18 = 19 = 20	81, [82], (82)	34, [34], (34)
	13 = 15	126, [119], (123)	193, [188], (176)				
	N	–, –, –	–, –, –		14	80, [80], (80)	33, [30], (29)
N.3	21 = 26 = 27 = 28 = 29 = 30	137, [137], (137)	181, [182], (182)	B.3	21 = 22 = 25 = 26 = 27 = 28 = 29 = 30	81, [81], (81)	33, [33], (33)
	22 = 25	134, [135], (135)	185, [184], (183)		23 = 24	75, [61], (60)	49, [72], (68)
	23 = 24	128, [117], (119)	197, [191], (183)				
N.4	31 = 32 = 33 = 35 = 36 = 37 = 38 = 39 = 40	104, [104], (104)	231, [231], (231)	B.4	31 = 32 = 33 = 35 = 3637 = 38 = 39 = 40	84, [84], (84)	34, [34], (34)
	34	101, [98], (98)	232, [229], (229)		34	81, [68], (67)	47, [66], (61)

[a] In each row, the first number is for C-doped, the second one for Si-doped and the third one for Ge-doped forms of (10, 0) BNNTs.

Table 4 The NMR parameters of C, Si and Ge-substituted (S_B) BNNTs.

Layers	Nuclei	ICS[a] (ppm)	ACS[a] (ppm)
N.1	1 = 2 = 3 = 4 = 5 = 6 = 7 = 8 = 9 = 10	167, [167], (167)	74, [74], (74)
N.2	11 = 15 = 16 = 17 = 18 = 19 = 20	139, [140], (140)	174, [174], (174)
	12 = 14	143, [138], (137)	170, [175], (173)
	13	142, [138], (139)	170, [160], (155)
N.3	21 = 24	140, [138], (138)	177, [178], (173)
	22 = 23	124, [132], (90)	124, [128], (164)
	25 = 26 = 27 = 28 = 29 = 30	136, [137], (137)	181, [181], (181)
N.4	31 = 35	105, [104], (104)	231, [231], (232)
	32 = 34	113, [104], (103)	231, [225], (224)
	33	84, [110], (76)	203, [199], (228)
	36 = 37 = 38 = 39 = 40	103, [104], (104)	230, [231], (231)
B.1	1 = 4	73, [72], (71)	47, [47], (47)
	2 = 3	78, [74], (75)	41, [45], (42)
	5 = 6 = 7 = 8 = 9 = 10	73, [73], (73)	47, [48], (48)
B.2	11 = 15 = 16 = 17 = 18 = 19 = 20	81, [82], (82)	34, [34], (34)
	12 = 14	83, [82], (83)	31, [30], (28)
	13	–, –, –	–, –, –
B.3	21 = 24 = 25 = 26 = 27 = 28 = 29 = 30	81, [81], (81)	32, [32], (32)
	22 = 23	83, [81], (80)	30, [32], (31)
B.4	31 = 32 = 33 = 34 = 35 = 36 = 37 = 38 = 39 = 40	84, [85], (85)	34, [34], (34)

[a] In each row, the first number is for C-doped, the second one for Si-doped and the third one for Ge-doped forms of (10, 0) BNNTs.

Table 5 The ^{11}B and ^{15}N natural charges.

Nuclei	Pristine	S_N[a]	Nuclei	Pristine	S_B[a]
B.34	1.147	0.974, [0.570], (0.633)	N.22	−1.197	−0.970, [−1.362], (−1.292)
B.23	1.194	1.000, [0.571], (0.625)	N.23	−1.197	−0.970, [−1.362], (−1.292)
B.24	1.194	1.000, [0.571], (0.625)	N.33	−1.189	−0.927, [−1.370], (−1.304)
N.3	−1.144	−1.125, [−1.144], (−1.157)	B.22	1.194	1.178, [1.192], (1.189)
N.4	−1.144	−1.125, [−1.144], (−1.157)	B.23	1.194	1.178, [1.192], (1.189)
N.13	−1.201	−1.178, [−1.195], (−1.199)	B.12	1.191	1.181, [1.185], (1.176)
N.15	−1.201	−1.178, [−1.195], (−1.199)	B.14	1.191	1.181, [1.185], (1.176)
N.23	−1.189	−1.184, [−1.200], (−1.208)	B.2	0.851	0.806, [0.832], (0.827)
N.24	−1.189	−1.184, [−1.200], (−1.208)	B.3	0.851	0.806, [0.832], (0.827)

[a] In each row, the first number is for C-doped, the second one for Si-doped and the third one for Ge-doped forms of (10, 0) BNNTs.

^{15}N nuclei. In both S_N and S_B models of Ge-doped BNNTs, the ICS values at the site of ^{15}N and ^{11}B nuclei decreased more than C- or Si-doped models, which follow the decreasing bond angles trend. With respect to the pristine BNNT, the variations of bond angles for C-doped BNNT in the S_N model are smaller than those of Si-doped. In the C-doped BNNT, the changes of the ICS values at the sites B.23, B.24 and B.34 are (as compared to the pristine model) smaller than the Si-doped BNNT but this trend is reversed at the sites of N.22, N.23 and N.33 in the S_B model (See Tables 1, 3 and 4). Table 5 lists the natural charges on substituted B and N sites by C, Si, or Ge atoms. It is shown that the change in natural charges on the sites of B.34, B.23, and B.24 substituted BNNTs are larger for doping with Si, Ge than it is with C dopant. The substitution of N sites changed the natural charges minutely.

4. Conclusion

We have calculated NMR parameters (ICS and ACS) at the site ^{11}B and ^{15}N nuclei of BN nanotubes doped with a carbon, silicon or a germanium atom for the first time. After optimization and calculations of ICS and ACS parameters, some trends were observed: (1) going from C to Si and to Ge atom, bond lengths increase but bond angles decrease for those atoms directly connected to C, Si or Ge. (2) In the Si and Ge-doped BNNT, the local symmetry of the tube breaks up after relaxation since the Si and Ge form a tetrahedral structure with the three nearest-neighboring atoms and they extend outward as compared to a normal BN nanotube. (3) In the pristine model of (10, 0) BNNT, the NMR parameters are divided into equivalent layers, among which the B.1 (B-mouth) has the smallest ICS but the N.1 (N-mouth) has the largest ICS among the B and N layers. Therefore, B.1 layer has the lowest electronic density and N.1 layer has the highest- the two layers can respectively act as electron acceptor and electron donor. (4) In the S_N substitution models, the NMR parameters of those B atoms that are directly connected to a C, Si or Ge and also those Ns that are directly connected to B (C or Si or Ge bonded) show significant changes; their ICS values have reduced and their ACS values have increased while those of the remaining atoms remain fairly unchanged. (5) In the S_B substitution models, the NMR parameters of those N atoms that are directly connected to a C, Si or Ge atom significantly changes; both their ICS and ACS values have reduced with respect to other nuclei. (6) In both S_N and S_B substitutions models, the ICS parameters of those B atoms directly connected to a Ge atom (S_N model) and also those of N atoms directly joined to a Ge atom (S_B model) are minimum in comparison to C and Si-doped BNNTs.

References

Becke, A.D., 1993. J. Chem. Phys. 98, 5648.

Bengu, E., Marks, L.D., 2001. Phys. Rev. Lett. 86, 2385.

Blase, X., Rubio, A., Louie, S.G., Cohen, M.L., 1994. Phys. Rev. B 51, 6868.

Boshra, A., Seif, A., 2009. Can. J. Phys. 87, 647.

Bovey, F.A., 1988. Nuclear Magnetic Resonance Spectroscopy. Academic Press, San Diego.

Chopra, N.G., Luyken, R.J., Cherrey, K., Crespi, V.H., Cohen, M.L., Louie, S.G., Zettle, A., 1995. Science 269, 966.

Czerw, R., Webster, S., Carroll, D.L., Vieira, S.M.C., Birkett, P.R., Rego, C.A., Roth, S., 2003. Appl. Phys. Lett. 83, 1617.

Frisch, M.J., et al., 2004. Gaussian 03, Revision C.01. Gaussian, Inc., Wallingford, CT, p. 255.

Golberg, D., Bando, Y., Han, W., Kurashima, K., Sato, T., 1999. Chem. Phys. Lett. 308, 337.

Goze Bac, C., Latil, S., Vaccarini, L., Gaveau, P., Tahir, S., Micholet, V., Aznar, R., Rubio, A., Metenier, K., Beguin, F., 2001. Phys. Rev. B 63, 100302.

Hayashi, S., Hoshi, F., Ishikura, T., Yumura, M., Ohshima, S., 2003. Carbon 41, 3047.

Iijima, S., 1991. Nature (London) 354, 56.

Loiseau, A., Willaime, F., Demoncy, N., Hug, G., Pascard, H., 1996. Phys. Rev. Lett. 76, 4737.

Parr, R.G., Yang, W., 1989. Density-Functional Theory of Atoms and Molecules. Oxford University Press, Oxford.

Saito, R., Dresselhaus, G., Dresselhaus, M.S., 1998. Physical Properties of Carbon Nanotubes. Imperial College Press, London.

Schleyer, P., Marker, C.J., 1996. Am. Chem. Soc. 118, 6317.

Seif, A., Boshra, A., 2009. J. Mol. Struct. 895, 82.

Si, M.S., Xue, D.S., 2006. Eur. Phys. Lett. 76, 664.

Tang, X.-P., Kleinhammes, A., Shimoda, H., Fleming, L., Bower, K.Y., Zhou, O., Wu, Y., 2000. Science 288, 492.

Wu, J., Zhang, W., 2008. Chem. Phys. Lett. 457, 169.

Wu, R.Q., Liu, L., Peng, G.W., Feng, Y.P., 2005. Appl. Phys. Lett. 86, 122510.

Xiang, H.J., Yang, J., Hou, J.G., Shizhu, Q., 2003. Phys. Rev. B 68, 035427.

Xin, C., Jing, M., Zheng, H., Qiang, W., Yi, C., 2005. J. Am. Chem. Soc. 127, 7982.

Zhang, M., Su, Z.M., Yan, L.K., Qiu, Y.Q., Chen, G.H., Wang, R.S., 2005. Chem. Phys. Lett. 408, 145.

Zurek, E., Pickard, C.J., Autschbach, J., 2007. J. Am. Chem. Soc. 129, 4430.